NANOCAT
NANOTECHNOLOGY AND CATALYSIS RESEARCH CENTRE

Malaysian Catalysis
An International Journal

Preface

This journal was initiated in 2019 with full enthusiasm by a group of personals in NANOCAT with a vision to provide a new platform for the latest advancement in catalysis research, exchange and stimulate the cross-fertilization of seminal ideas and to facilitate the rapid dissemination of frontier research. The journal was named Malaysian Catalyst – An International Journal (MCIJ) for the purpose of giving a distinct and unique local identity but nevertheless its open to the international arena where scientist and researches all over the world are welcome to contribute. We have been through tremendous challenges during initial days to formulated and conceptualized the idea of this journal while processing for the paper submission, evaluation, formation and production. However, despite all the challenges, we are ready to publish the inaugural first volume. MCIJ aim to be the premier scholarly publication in the field of catalysis and an indispensable source of information for scientist and engineers in both industrial and academic fields. It is an international open access journal of catalysts. Our aim is to encourage scientists to publish their experimental and theoretical results in as much detail as possible. MCIJ publishes original, rigorous, and scholarly contributions in the fields of homogeneous and heterogeneous catalysis, bio related catalysis including studies that relate catalytic function to fundamental chemical processes at surfaces and in metal complexes, novel concepts in surface chemistry, the synthesis and catalytic function of novel inorganic solids and complexes, spectroscopic methods for structural characterization, and theoretical methods of direct interest and impact in the science and applications of catalysts and catalytic processes. MCIJ also publishes review articles, news and views, research highlights about important papers published in other journals, commentaries, book reviews, correspondence, commercialization, ethical and social issues. In this way, the journal aims to be the premier voice of the worldwide catalysis community. MCIJ offers readers and authors high visibility, access to a broad readership, high standards of copy editing and production, rigorous peer review, rapid publication, and independence from academic societies and other vested interests. MCIJ provides authors with high quality, helpful reviews that are shaped to assist authors in improving their manuscripts. I very much appreciate your support as we strive to make MCIJ the most authoritative journal in catalysis.

Editor-in-Chief

Professor Dr. Mohd Rafie Johan

Editorial Team

Table of Content

Malaysian Catalysis-An International Journal

Malay. Catal. Int. J Vol 1 (2021) 1-14

RESEARCH ARTICLE

Impact of TiO_2 content on Titanium oxide supported chitosan photocatalytic system to treat organic dyes from wastewater

Received 14th Dec 2020,
Revised 04th May 2021,
Accepted 10th May 2021

DOI: 10.22452/mcij.vol1no1.1

Corresponding author :
nurhidayatullaili@um.edu.my

Muhammad Nur Iman Amir [a], Nurhidayatullaili Muhd Julkapli[a*], and Saba Afzal[b]

[a] Nanotechnology and Catalysis Research Centre (NANOCAT), 3rd Floor Block A, Institute for Advanced Studies, Universiti Malaya, 50603 Kuala Lumpur, Malaysia

[b] Department of Chemistry, Sardar Bahadur Khan Women's University, Quetta, Pakistan

Abstract

Titanium dioxide (TiO_2) nanoparticles are used enormously for treating wastewater pollutants due to their unique optoelectronic and physiochemical properties. Though, wide bandgap, fast recombination of e^- - h^+ pair, and low adsorption toward organic pollutants limit their applications. However, immobilization of TiO_2 on Chitosan (Cs) is believed to overcome these limitations. Cs with plenty of NH_2 and OH groups in their structure are expected to enhance their adsorption and consequently photocatalytic performance. A series of TiO_2/Cs photocatalysts have been prepared using a chemical co-precipitation method. Amount of TiO_2 is varied from 0.25, 0.50, and 0.75 to 1.0 g. The photocatalysts are characterized by using FESEM-EDS, CHNS Elemental Analyser TGA, FTIR, and UV-Vis spectroscopy. These characterization results revealed the formation of a good interface between TiO_2 and Cs matrix. Increasing TiO_2 content significantly increased the thermal stability of the photocatalyst up to 600°C. The photocatalytic activity of Cs/TiO_2 is observed under UV light which is found to be more significant with 1:1(TiO_2: Cs) composition for the degradation of methylene blue dye at 85 % and be maintained up to 4 numbers of cycles. This demonstrated open new insight into the application of Cs as a support materials and adsorption agent in TiO_2 based photocatalyst system

Keywords: Chitosan; Titanium dioxide; adsorption; Photodegradation; Methylene blue

1. Introduction

Wastewater pollution arises significantly during the past few decades due to increasing industrialization such as textile, packaging, dyeing, and plastic industries. Heavy metal ions, hormones, pathogen, aromatic compounds (including phenolic derivatives and polycyclic aromatic compounds), and dyes are added into the water stream as a pollutant [1-5]. Although waste discharge from industries has to be limited to 5 % of polluted water this percentage is still alarming for human and aquatic life [6]. Due to the shortage of freshwater supplies, wastewater needs to be treated to ensure the availability of clean and safe water to use.

Many techniques introduced to treat polluted water, however, conventional methods like coagulation, flocculation, sedimentation, ultrafiltration and reverse osmosis [7-8] are not very effective due to non-biodegradability and chemical stability of pollutants [3;6]. Furthermore, some of these techniques generate huge amounts of sludge, increasing the cost of separation [2;4]. Alternatively, advanced oxidation procedures like photocatalysis utilizing semiconductor molecules gain special interests as it has a strong tendency towards pollutant degradation. This is due to the generation of electron-hole pairs by the illumination of light (UV or Vis) equal or greater than their bandgap energy of semiconductors, producing reactive species like H_2O_2, OH, and $O_2^{\cdot}$ [6;9] (Figure 1). These reactive species degrade pollutant molecules into less harmful CO_2, H_2O, and H_2 (1,3).

Among semiconductors, TiO_2 is widely utilized for the treatment of wastewater due to its photo-stability, chemically/biologically inertness [5-8] and availability, and low cost [10-12]. However, electron-hole recombination, difficult separation, and agglomeration at higher loading are some properties that limit the applications of TiO_2[11;13]. These series of limitations can be overcome by introducing some support such as natural or synthetic fabrics, polymer membranes, activated carbon, quartz, glass, optical fibers, zeolites, aluminum, stainless steel, and titanium metal [14-16]. Support material must have strong surface bonding characteristics with catalyst, high specific surface area, good adsorption capability, high separation ability, and chemically inert [15].

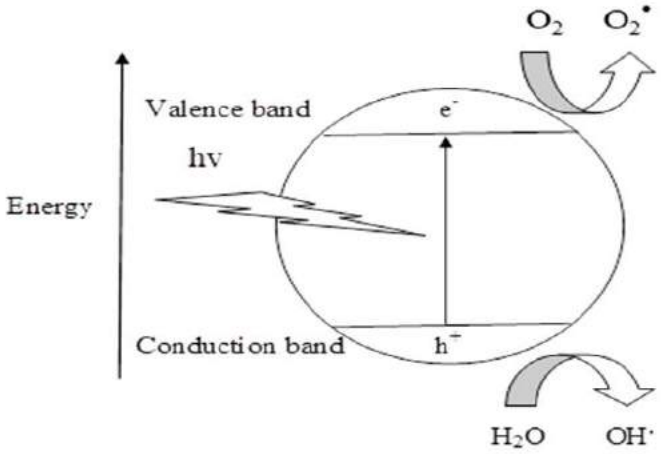

Figure 1. Photocatalytic mechanism of semiconductors for photodegradation of synthetic compounds

Chitosan (Cs) is a type of natural polymer found abundantly and has the potential to use as a support material [17-19]. It contains plenty of NH_2 and OH groups in its structure (Figure 2), which gives specials properties to the Chitosan [18;20]. It can be used extensively as a support for the preparation of heterogeneous catalysts in the form of colloids, flakes, gel, and beads [21-22]. The promising hydrophilic character of Cs is due to the large number of OH groups gave advantages in absorption properties. Besides that, Cs will prevent TiO_2 from agglomeration and make the separation process more efficient.

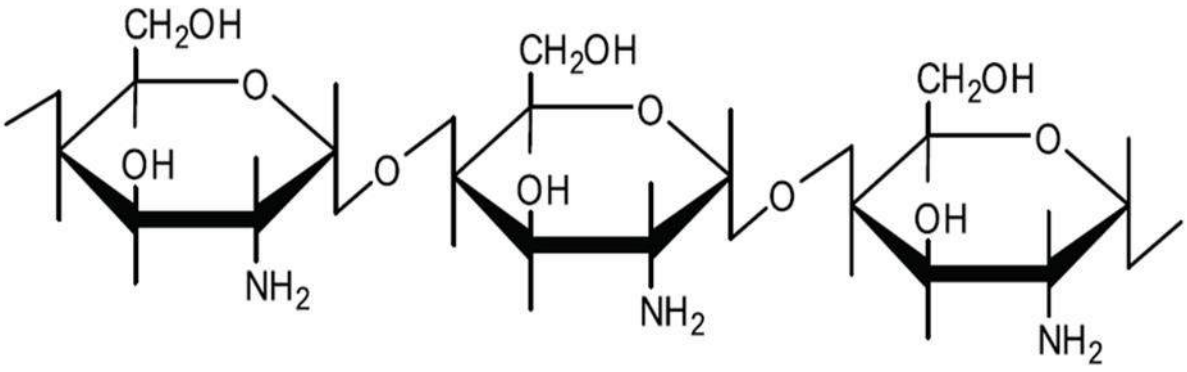

Figure 2. Chemical configuration of Cs biopolymer

The present work aims to synthesis Cs-TiO_2 photocatalyst by varying concentrations of TiO_2 to achieve the best ratio of Cs-TiO_2 photocatalyst. It is expected that the optimized photocatalyst is thermally more stable and gives better interactions between TiO_2-Cs matrix and performs efficiently in the photodegradation process.

2. Methodology

2.1. Preparation of TiO_2/Cs photocatalyst

TiO_2/Cs photocatalyst beads were prepared by using the chemical co-precipitation method. Cs solution is prepared by dissolving 1g CS in acetic acid followed by the addition of TiO_2 powder (0.25, 0.5, 0.75, and 1.0 g) with continuous stirring of 24 hours. The as-prepared TiO2/CS solution is sprayed into a precipitation bath containing NaOH (500 ml; 1.5 M). The NaOH solution neutralizes the acetic acid within the Cs gel and is transformed into spherical uniform gel beads. The wet TiO_2/Cs gel beads were rinsed with distilled water to remove NaOH residues. The beads are filtered and air-dried for about 30 min/h.

2.2. Characterization

The photocatalyst TiO2/CS is characterized using various characterization techniques such as FTIR analysis is carried out using Perkin-Elmer Instrument (model FTIR spectrum 400) to determine the functional groups present on TiO_2/Cs photocatalyst. The samples (2mg) are mixed with Potassium Bromide (KBr) powder (98 mg) ground and compressed at 400 psi to produce thin films. Thermogravimetric analysis is performed on a Perkin-Elmer Pyris 1 TGA Analyzer (25°C to 650°C at 10°Cmin^{-1}) in a nitrogen atmosphere to determine the weight loss percentage over temperature. Elemental analysis is conducted using CHNS Elemental Analyzer 2 (Perkin-Elmer) to provide information on the carbon, nitrogen, and hydrogen element content of the sample.

2.3. Adsorption–photodegradation Activity

Photocatalytic tests were conducted under a UV lamp (96 Watt) provided with an air pump to ensure the continuous supply of oxygen. 10 ppm of MB solution is filled in a quartz tube and catalyst loading (TiO_2/Cs photocatalyst) set at 0.01 g. Before the UV light exposure, the solution is placed under the dark for 30 min to set adsorption-desorption equilibrium. The aliquots of 3 mL are taken at the 15 min interval for analyzing adsorption photodegradation by UV-Vis

spectroscopy. After the photodegradation process, an MB solution is centrifuged for 15 min at 3000 rpm to separate the beads and solution. The recycling activities of the photocatalyst have been done according to the optimum composition of TiO_2: Cs with optimum experimental conditions.

3. Results and discussion

3.1. FESEM-EDS analysis

The morphology and homogeneity of TiO_2 nanoparticles within the Cs matrix are analyzed using FESEM. SEM micrographs of the photocatalysts at varying TiO_2 weight ratios are shown in Figure 3. Furthermore, the elemental composition of all the synthesized photocatalysts at varying TiO_2 ratios is determined using EDS. SEM micrographs of all photocatalysts demonstrated that spherical TiO_2 nanoparticles disperse uniformly; however, the uniformity and homogeneity increase as the weight ratio of TiO_2 increases as obvious from Figure 3d. It indicated that TiO_2 and CS with identical wt. ratios give good homogeneity of the photocatalyst. Furthermore, EDS analysis indicated the presence of Ti, O, N and C elements which suggest the presence of TiO_2 and its incorporation with the Cs matrix [5-9]. The presence of N suggests that the possible interactions between metal oxides (TiO_2) are with the NH_2 group of Cs [17].

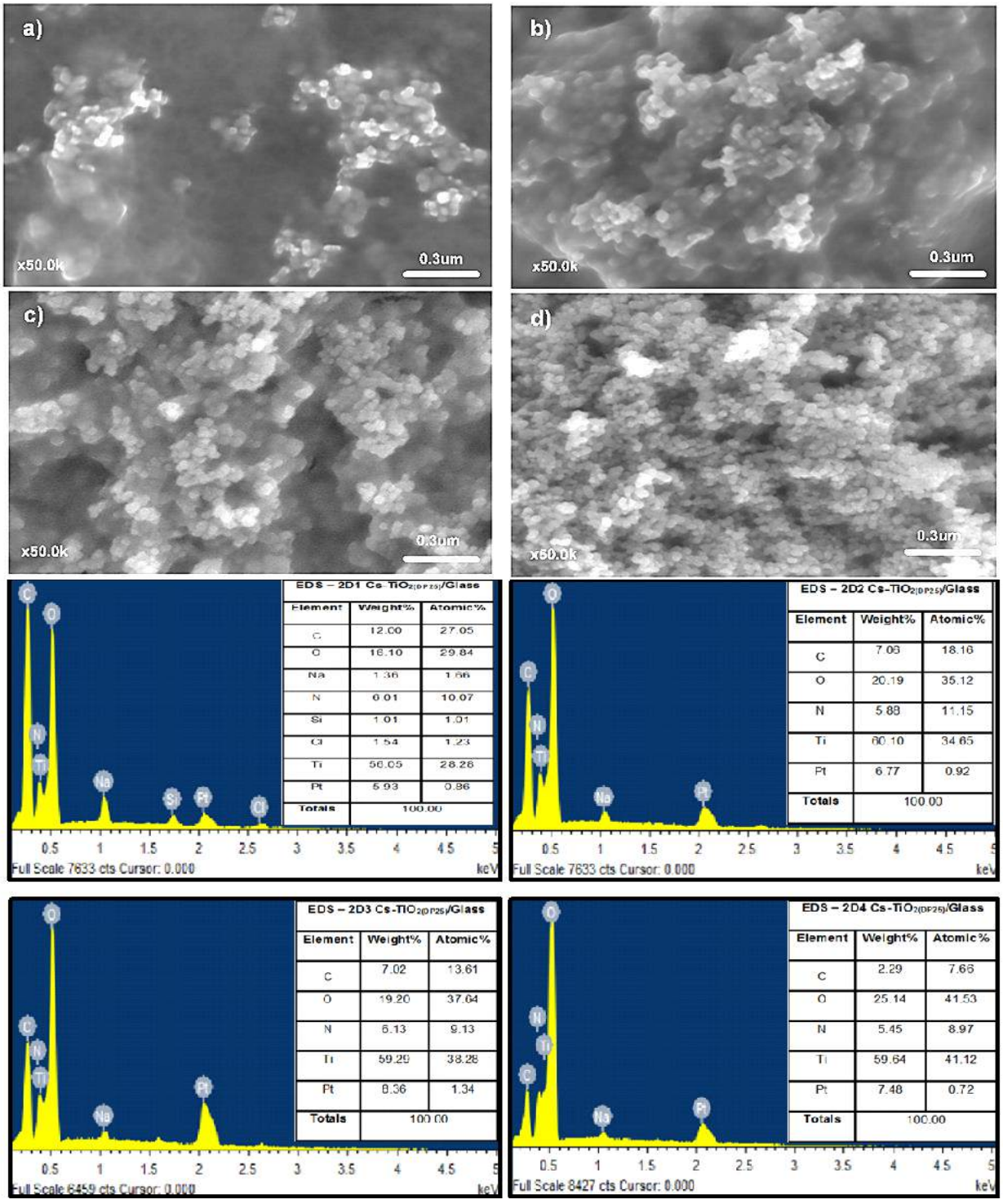

Figure 3. FESEM-EDS micrographs of TiO_2/Cs with weight ratio of (a) 1.0:0.25 (b) 1.0:0.5 (c) 1.0:0.75 and (d) 1.0:1.0

3.2. Elemental analysis

Figure 4 demonstrated the EA results of the TiO_2/Cs photocatalyst system on varying TiO_2 content. It is evident from the bar diagrams that as the concentration of TiO_2 increases the percentage of C, H, and N elements gradually decreased as CS is an organic polymer and these elements play a vital role in the bonding interactions with metal oxides [18-19]. Therefore, the gradual decrease of these elements indicates the successful synthesis of TiO_2/Cs photocatalyst at varying TiO_2 content; however, the overall bonding interaction is confirmed further by using other characterization techniques, including FTIR.

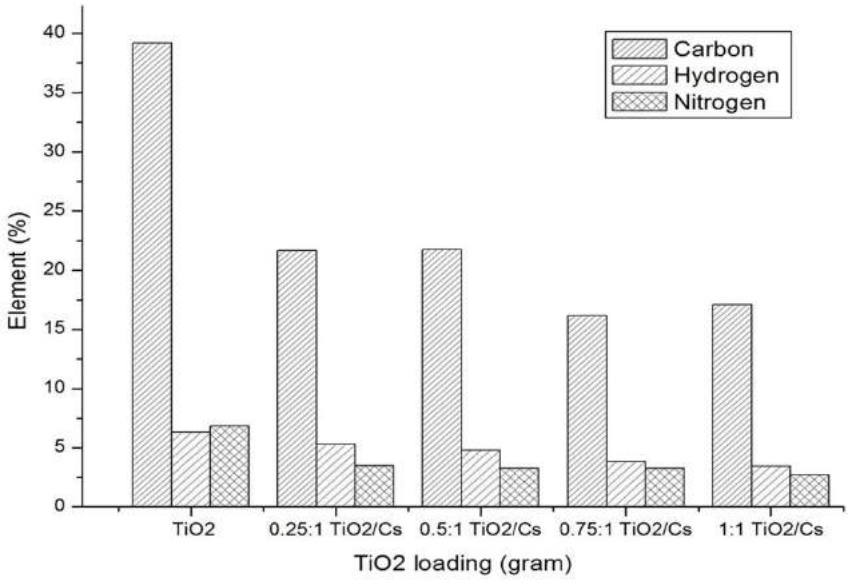

Figure 4. The elemental composition of TiO_2/Cs photocatalyst

3.3. Thermogravimetry Analysis

Thermogravimetry analysis (TGA) of TiO2/Cs photocatalyst at different TiO_2 is shown in Figure 5. As observed from the thermograms, all samples showed an almost similar pattern with three stages of decomposition except pure TiO_2 which shows single-step degradation. The first degradation occurred between 50 °C to 100 °C which was attributed to the removal of moisture. This might be due to the hydrophilic characteristic of Cs [12]. The second degradation was observed between 135 °C to 200 °C due to the decomposition of organic content Cs [19]. The third

degradation step occurred around 600 °C due to metal oxide and after that, no prominent degradation is observed. The sample with lower TiO_2 content degrades earlier as organic compounds (Cs) thermally less stable. The addition of TiO_2 into Cs increases its thermal stability [16-19]. Therefore, the thermal stability of TiO_2/Cs is linearly increased with the content of TiO_2. The weight loss percent went up to 56 % for pure Cs, 53.9 % (0.25 g), 37.4 % (0.5 g), 33.1 % (0.75 g) and 26.2 % (1.0 g). The amounts of TiO_2 in the samples can estimate from the residual mass percentages that are 24, 28, 40, and 45 % as increased TiO_2 loading from 0.25 until 1.0 g.

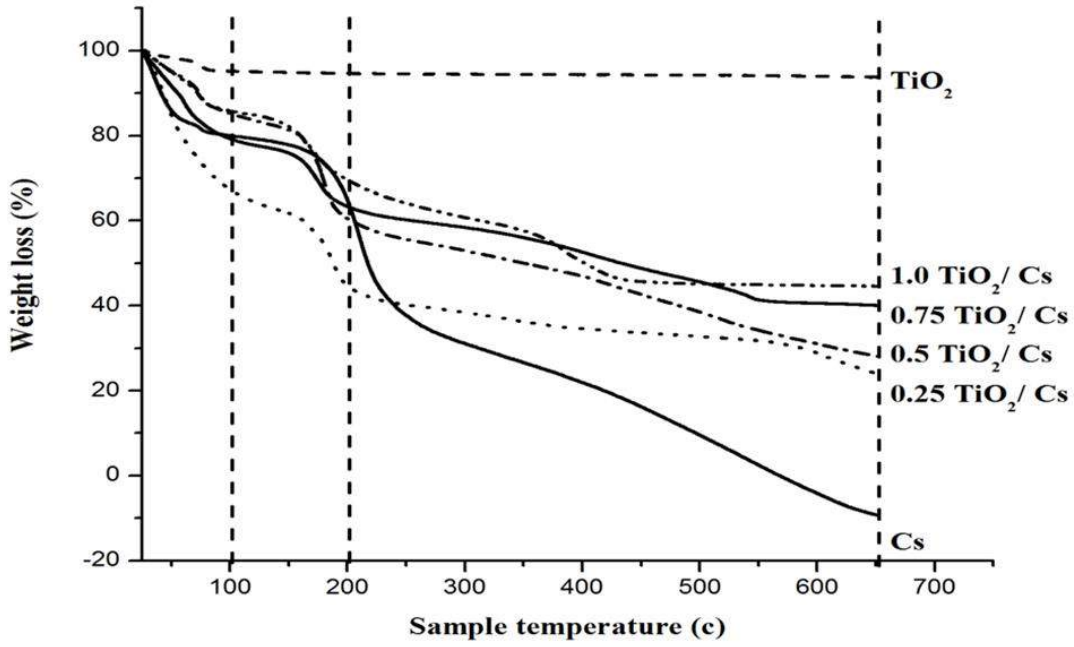

Figure 5. The thermal degradation of TiO_2/Cs photocatalysis (35 to 600℃)

3.4. Fourier Transform Infra-Red (FTIR) analysis

The composition of photocatalysts and bonding interactions between a metal oxide and Cs is further confirmed through FTIR (Figure 6). The FTIR spectra of all the photocatalysts showed almost similar patterns with a prominent variation in peak intensity. The peak in the range of 3450 cm^{-1} is attributed to NH_2 and OH groups of the Cs network. Literature shows the presence of Inter and intra-molecular hydrogen bonding co-existed at this range [19, 20]. The peak in the range of 1661cm^{-1} corresponds to the bending vibration of the N-H group. Stretching vibration from C-O groups is observed at 1393cm^{-1}. The characteristic peak of the C-N group of Cs is observed at 1156

cm^{-1}. For raw TiO_2, a prominent signal was observed at 580 cm^{-1} that corresponds to the O-Ti-O bond [3;5]. The FTIR spectra show a gradual decline in peak intensities (1661, 1393, 1156cm^{-1}) as the TiO_2 content increases. This might be due to the less availability of free NH and OH groups of CS and their involvement in bonding with metal oxide (TiO_2) [10-13]. Hence the sample with a 1:1 ratio of Cs-TiO_2 shows better interactions and expected to perform well in the photocatalytic process.

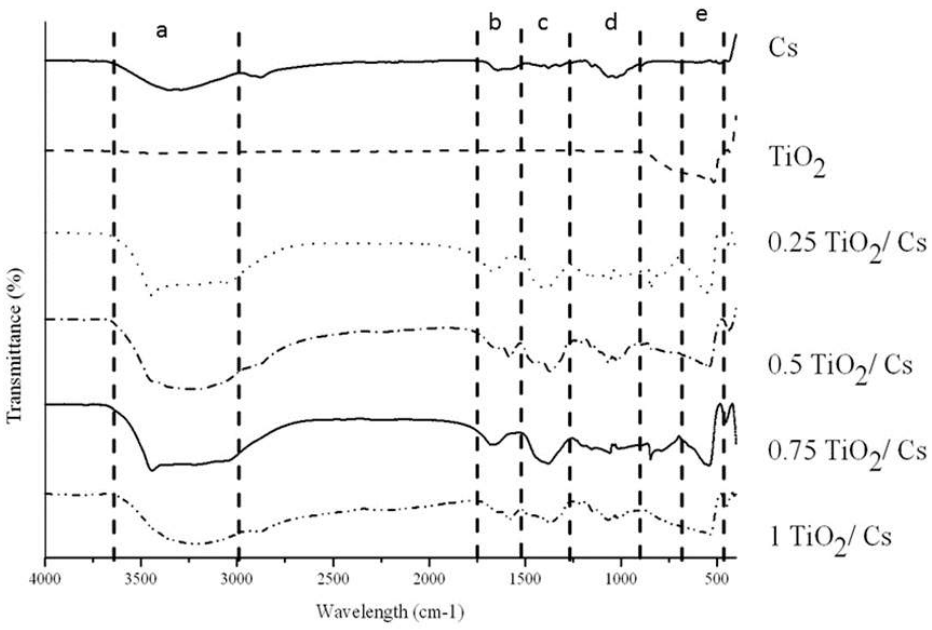

Figure 6. The FTIR spectrum of TiO_2/Cs at different compositions of TiO_2 nanoparticles

3.5. Photocatalytic Activity

The photocatalytic performance of all the composite samples is assessed by degradation of the MB as a model pollutant under UV light. Figure 7 shows that comparing other photocatalyst TiO_2/Cs with a 1:1 ratio shows the complete decolorization of dye solution within 2h of UV light exposure. This was due to the high amount of TiO_2 which is responsible for the contribution of more free electrons and holes to undergo a faster degradation process. It can also be attributed that the equal ratio of TiO_2 and Cs gives better interactions which consequently minimize the recombination of electrons and holes, and photocatalyst performs well in the degradation process [12-14].

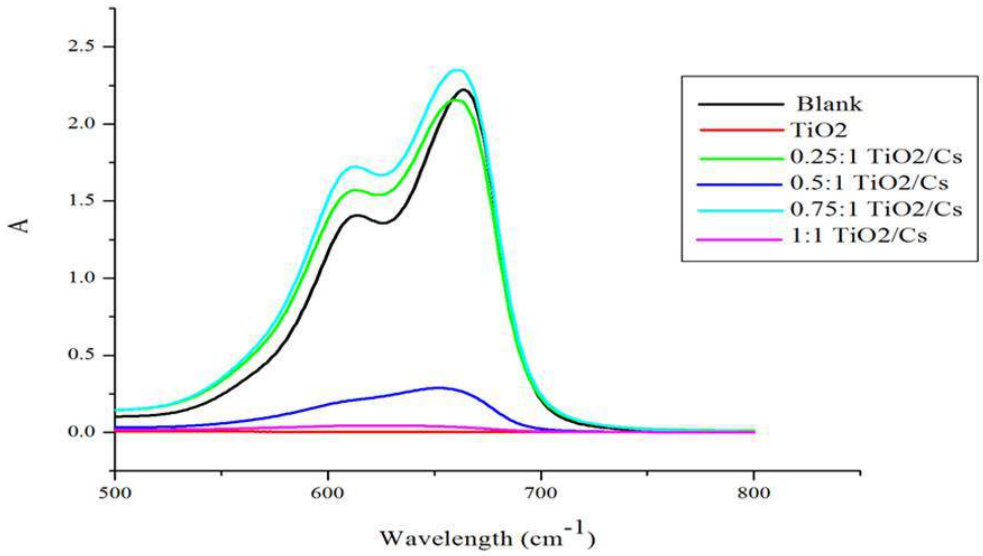

Figure 7. The decolorization of MB by TiO_2/Cs under UV Vis spectroscopy analysis

Furthermore, an illustration of the mechanism of MB photodegradation over TiO_2/Cs photocatalyst is represented in Figure 8 *viz* the whole photodegradation process, from the adsorption of MB dye molecules on the surface of the photocatalyst to the decomposition of MB molecules by reactive radicals by TiO_2. The degradation of MB does not necessarily correspond to the oxidation and mineralization of the molecule, and the reduced form of MB which is colorless has been produced in the presence of light [9-12]. The lack of coincidence among the best performing samples concerning either decolorization or mineralization has been the result of different routes followed by MB during irradiation.

The MB molecule can be transformed into Leuco MB through reduction by electrons in the conduction band or oxidized by interactions with the valence band holes or native OH species, starting with a de-methylation step to be finally mineralized. For long reaction times also Leuco MB can be further degraded and mineralized [11].

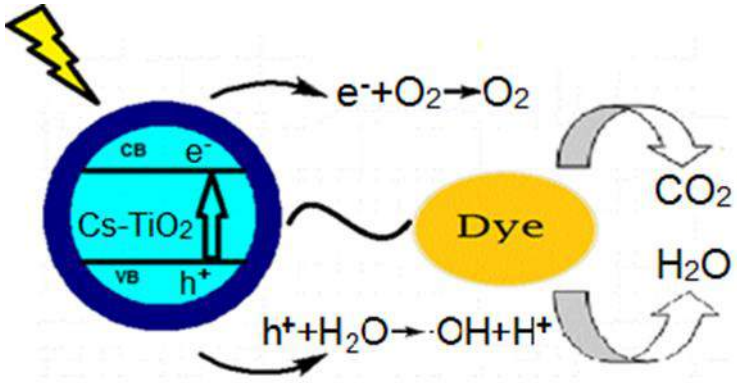

Figure 8. Photodegradation mechanism of MB dye over TiO_2/Cs photocatalyst

3.6. Photocatalyst recovery and reusability

To evaluate the performance of TiO2/Cs for environmental applications, the reusability test was performed for four catalytic cycles and the results are presented in Figure 9. After completing MB degradation, the TiO_2/CS sample was collected and utilized for the next cycle under optimal conditions. The reusability results indicated that after four consecutive runs, the removal of MB by the TiO_2/CS sample still reached 87-89 % within two hours of light exposure, indicating that there is a slight reduction in the catalytic activity of the TiO_2/CS. The interactions between the constituent elements of TiO_2/CS are sufficient to maintain its morphological and optical properties during the degradation process. As a result, the composite sample can be used effectively for wastewater treatment.

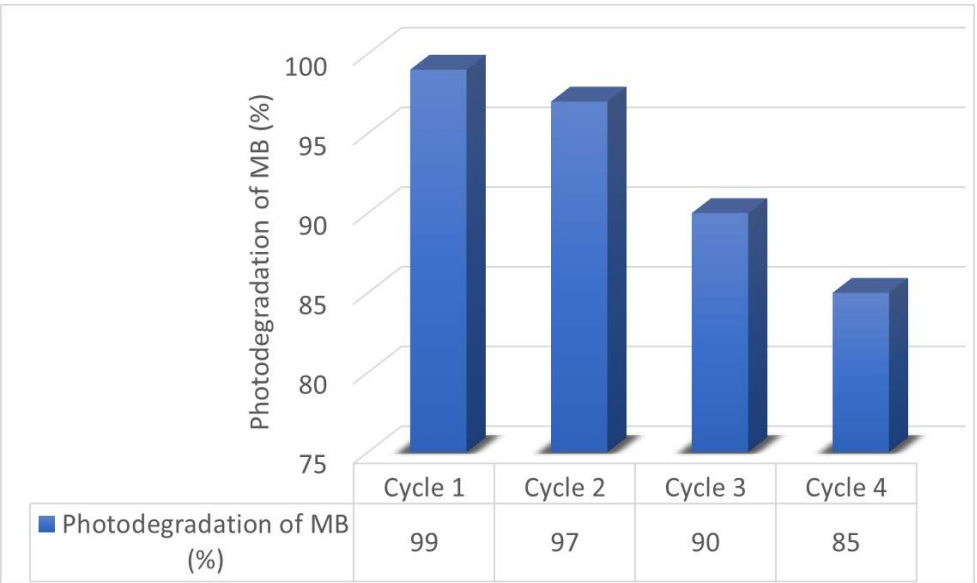

Figure 9. Reusability data over TiO_2/CS in degradation of MB UV light

Conclusion

The present work reports the synthesis of TiO_2/Cs photocatalyst on varying TiO_2 concentrations. Characterization results indicate that the photolysis with the identical ratio of Cs and TiO_2 is thermally more stable than samples with lower TiO_2 content. Similarly, TiO_2/Cs (1:1) shows the better interactions between TiO_2 and polymer Cs as expressed from FTIR results which further corresponds to its higher degradation rates towards MB dye. Thus, the work provides a base for understanding the significance of metal oxide concentration in synthesizing photocatalyst systems and its application towards the photodegradation of various wastewater pollutants.

Acknowledgement

This work was financially supported by the University Malaya Research Grant (UMRG RP044A-17AET) and Postgraduate Research Fund (PG239-2015A), Universiti Malaya.

References

1. Z. Shayegan, C.S. Lee, F. Haghighat. TiO_2 photocatalyst for removal of volatile organic compounds in gas phase–A review. *Chem. Eng. J.* **2018**, 334, 2408-2439.
2. D. Gao, X. Wu, P. Wang, Y. Xu, H. Yu, J. Yu, Simultaneous realization of direct photoinduced deposition and improved H_2-evolution performance of Sn-nanoparticle-modified TiO_2 photocatalyst. *ACS Sustain. Chem. Eng*. **2019**, 7(11), 10084-10094.

3. H. Abdullah, M. M. R. Khan, H. R. Ong and Z. Yaakob. Modified TiO_2 photocatalyst for CO_2 photocatalytic reduction: an overview. *J. CO2 Util.* **2017**, 22, 15-32.
4. Y. Yang, L. C. Yin, Y. Gong, P. Niu, J.Q. Wang, L. Gu, X. Chen, G. Liu, L. Wang, and H.M. Cheng. An unusual strong visible-light absorption band in red anatase TiO2 photocatalyst induced by atomic hydrogen-occupied oxygen vacancies. *Adv. Mater*, **2018**, 30(6), 1704479
5. D. Gao, W. Liu, Y. Xu, P. Wang, J. Fan and H. Yu, Core-shell Ag@Ni cocatalyst on the TiO_2 photocatalyst: one-step photoinduced deposition and its improved H_2-evolution activity. *Appl. Catal. B.* **2020**, 260, 118190.
6. M. S. F. A. Zamri, N. Sapawe Regeneration studies of TiO_2 photocatalyst for degradation of phenol in a batch system. Mater. Today: Proc. **2019**, 19, 1327-1332.
7. B.A Bhanvase, T.P. Shende, S.H. Sonawane. A review on graphene–TiO_2 and doped graphene–TiO2 nanocomposite photocatalyst for water and wastewater treatment. *Environ. Technol. Rev.* **2017**, 6(1), 1-14.
8. J. Hu, S. Zhang, Y. Cao, H. Wang, H. Yu, F. Peng Novel highly active anatase/rutile TiO_2 photocatalyst with hydrogenated heterophase interface structures for photoelectrochemical water splitting into hydrogen. *ACS Sustain. Chem. Eng*, **2018**, 6(8), 10823-10832.
9. K. Shoueir, S. Kandil, H. El-hosainy, M. El-Kemary. Tailoring the surface reactivity of plasmonic Au@TiO_2 photocatalyst bio-based chitosan fiber towards cleaner of harmful water pollutants under visible-light irradiation. *J. Clean. Prod*. **2019**, 230, 383-393.
10. K. Shirai, G. Fazio, T. Sugimoto, D. Selli, L. Ferraro, K. Watanabe, M. Haruta, B. Ohtani, H. Kurata, C. Di Valentin and Y. Matsumoto.,. Water-assisted hole trapping at the highly curved surface of nano-TiO2 photocatalyst. *J. Am. Chem. Soc*, **2018**, 140(4),1415-1422.
11. M. Guo, W. Jiang, C. Chen, S. Qu, J. Lu, W. Yi and J. Ding. (2021). Process optimization of biodiesel production from waste cooking oil by esterification of free fatty acids using La^{3+}/ZnO-TiO_2 photocatalyst. *Energy Convers. Manage.* **2021**, 229, 113745.
12. L. Yi, F. Lan, J. Li, C. Zhao, Efficient noble-metal-free Co-NG/TiO_2 photocatalyst for H2 evolution: Synergistic effect between single-atom Co and N-doped graphene for enhanced photocatalytic activity. *ACS Sustain. Chem. Eng.* **2018,** 6(10), 12766-12775.
13. A. Abdelhaleem, W. Chu, X. Liang, Diphenamid degradation via sulfite activation under visible LED using Fe (III) impregnated N-doped TiO2 photocatalyst. *Appl. Catal. B.* **2019**, 244, 823-835.
14. F. Chen, P. Ho, R. Ran, W. Chen, Z. Si, X. Wu, D. Weng, Z. Huang and C. Lee, Synergistic effect of CeO2 modified TiO2 photocatalyst on the enhancement of visible light photocatalytic performance. *J. Alloys Compd*., **2017**, 714, pp.560-566.
15. H. L. Yu, Q. X. Wu, J. Wang, L. Q. Liu, B. Zheng, C. Zhang, Y. G. Shen, C. L. Huang, B. Zhou and J. R. Jia. Simple fabrication of the Ag-Ag_2O-TiO_2 photocatalyst thin films on polyester fabrics by magnetron sputtering and its photocatalytic activity. *Appl. Surf. Sci*. **2020,** 503, 144075

16. M. A. M. Adnan, B. L Phoon, N, N. M Julkapli. Mitigation of pollutants by chitosan /metallic oxide photocatalyst: a review. *J. Clean. Prod*. **2020**, 261, 121190.
17. S. Zarei, N. Farhadian, R. Akbarzadeh, M. Pirsaheb, A. Asadi, Z. Safaei,. Fabrication of novel 2D Ag-TiO_2/γ-Al_2O_3/Chitosan nanocomposite photocatalyst toward enhanced photocatalytic reduction of nitrate. *Int. J. Biol. Macromol*, **2020**, 145, 926-935.
18. A. M. Saad, M. R. Abukhadra, S. Abdel-Kader Ahmed, A. M. Elzanaty, A. H. Mady, M. A. Betiha, J. J. Shim and A. M. Rabie. Photocatalytic degradation of malachite green dye using chitosan supported ZnO and Ce–ZnO nano-flowers under visible light. *J. Environ. Manage*. **2020,** 258, .110043.
19. S. J. Shah, A. Khan, N. Naz, A. Ismail, M. Zahid, M. S. Khan, Awais, M. Ismail, S. u. H. Bakhtiar, I. Khan, B. Ahmad, N. Ali, A. Zada and S. Ali, Synthesis of CoCrFeO4-chitosan beads sun-light-driven photocatalyst with well recycling for efficiently degrading high-concentration dyes. *Spectrochim Acta A.* **2020,** 236, 118314.
20. I. H. Tseng, Z. C. Liu, P. Y. Chang, Bio-friendly titania-grafted chitosan film with biomimetic surface structure for photocatalytic application. *Carbohydr. Polym*. **2020,** 230, 115584.

Malaysian Catalysis-An International Journal

Malay. Catal. Int. J Vol 1 (2021) 15-25

RESEARCH ARTICLE

Poly(N-vinylimidazole): A biocompatible, efficient, and highly recyclable heterogeneous catalyst for the preparation of bis(3-indolyl) methanes

Hayedeh Gorjian,[a] Hoda Fahim,[a] and Nader Ghaffari Khaligh, [a,b]

[a] Department of Food Science and Technology, Sari Agricultural Sciences and Natural Resources University, Sari, Iran

[b] Nanotechnology and Catalysis Research Centre, Institute for Advanced Studies (IAS), University of Malaya, 50603 Kuala Lumpur, Malaysia

Received 20th May 2021
Revised 05th July 2021
Accepted 23rd July 2021

DOI: 10.22452/mcij.vol1no1.2

Corresponding author:
ngkhaligh@um.edu.my

Abstract

Poly(N-vinylimidazole) (PVIm), as a biocompatible, efficient, halogen-free, and reusable catalyst, was applied for the solvent-free synthesis of a library of bis(3-indolyl) methanes. The reaction was smoothly carried out under mild conditions, and the crude products were purified easily, and the pure products were obtained in high to excellent yields

Keywords: Heterogeneous catalysis, Functional Polymer, Multicomponent reaction, Bis(3-indolyl)methanes, Ball mill Solvent-free technique

1. Introduction

Indole and its natural and synthetic derivatives are important nitrogen-heteroaromatic scaffolds due to diverse biological properties in the drug synthesis and pharmaceutical industry [1-5]. Bis-indolylalkanes are an essential class of bioactive metabolites of terrestrial and marine origin [6-8]. They are active cruciferous ingredients that promote beneficial estrogen metabolism [9]. Owing to the significant and unique biological properties of BIMs, numerous methods and catalysts have been reported for their synthesis [10-12]. The catalytic synthesis of BIMs is often conducted by condensing two moles of indoles with one mole of carbonyl compound using a Brönsted or Lewis acid catalyst. Many homogeneous and heterogeneous catalysts have been reported for this

synthesis route in the literature [13-23]. It is well-known that nitrogen-based catalysts, reagents, and reactants can deactivate and/or decompose Lewis acids [23, 24]. However, Lewis acids are often expensive, and their use in stoichiometric amounts and large scale may not be economical.

Furthermore, the catalyst leakage in pharmaceutical processes can cause serious health problems for human beings. Some other drawbacks include the formation of by-products, prolonged reaction time, corrosion, and waste acid pollution problems [25, 26]. The research finds a safe and green methodology using stable and reusable catalysts under mild conditions to overcome the mentioned disadvantages and develop sound and green methods.

Functional polymers are macromolecules containing functional groups [27]. Poly(N-vinylimidazole) (PVIm) is a biocompatible [28], biodegradable [29], thermal stable [30], and water-soluble linear polymer with pKa around 6.0 [31]. PVIm, as a pH-sensitive functional polymer, can be protonated at acidic pH and de-protonated under basic conditions [32]. PVIm and its copolymers have been applied in the suppressing gene expression, as drug and protein delivery carriers [31], heavy metal removal via metal-binding chelating [33, 34], catalysis [35-38], pervaporation [39], fuel cell [40], CO2 separation [41], and nanofiltration separation [42].

2.0 Experimental

2.1 General procedure

The chemicals, reagents, and solvents were analytical grade and purchased from Sigma Aldrich, ACROS organic, Alfa Aesar, and Fisher Chemical Companies and used as purchased. The purity determination of the products was accomplished by TLC on silica gel polygram SIL G/UV 254 plates. The MS was measured under GC (70 eV) conditions. The IR spectra were recorded on a Perkin Elmer 781 Spectrophotometer. In all the cases, the 1H NMR spectra were recorded with Bruker Avance 400 MHz instruments. Chemical shifts are reported in parts per million in DMSO-d6 and CDCl3 with tetramethylsilane as an internal standard.

2.2 General Procedure for the Synthesis of BIMs

Poly(N-vinylimidazole) (PVIm) was fabricated through free radical polymerization of N-vinylimidazole in toluene at N2 atmosphere with azobisisobutyronitrile (AIBN) as the initiator [37]. The Mv value of PVIm was determined to be 302,000 g mol through viscometry using the Mark–Houwink–Sakurada equation [51]. PVIm (20 mg) was mixed and stirred at 80 °C with a

mixture of a carbonyl compound (1) (1 mmol) and indole (2a) or 2-methylindole (2b) (2 mmol) under solvent-free conditions. After appropriate reaction time (monitored by TLC), cold diethyl ether (30 mL) was added into the reaction mixture, and the catalyst was separated by simple filtration. Next, PVIm was washed with Et2O (5 mL) and acetone (5 mL) and dried at ambient temperature. The recovered PVIm was reused for the next run. The ethereal solution was dried at reduced pressure by a rotary evaporator, and the crude product was purified by recrystallization from a mixed solvent of ethanol: water (95:5 %). The physical and spectral data of the pure products were in good agreement with those previously reported in the literature [43].

2.3 Color, melting point, and ^{1}H NMR data of the selected products:

3r: Orange solid, m.p. = 243-244 °C; ^{1}H NMR (CDCl3, 400 MHz) δ = 8.80 (s, 3H), 8.35 (d, J = 7.8 Hz, 3H), 7.88 (s, 3H), 7.49-7.42 (d, J = 7.8 Hz, 3H), 7.38-7.34 (m, 6H), 6.14 (s, 1H) ppm.
3s: Pale yellow needles, m.p. = > 300 °C; ^{1}H NMR (CDCl3, 400 MHz) δ = 8.11 (s, 2H), 7.74 (s, 1H), 7.38-7.31 (m, 5H), 7.14 (dd, J = 7.6 and 8.0 Hz, 3H), 6.94-6.98 (m, 6H) ppm.
3f': Yellow solid, m.p. = 298-299 °C; ^{1}H NMR (DMSO-d6, 300 MHz) δ = 10.92 (s, 1H), 10.88 (s, 1H), 10.58 (s, 1H), 7.26-7.21 (m, 3H), 7.17 (d, J = 7.4 Hz, 1H), 6.94 (d, J = 7.6 Hz, 1H), 6.90-6.82 (m, 3H), 6.74 (d, J = 8.2 Hz, 1H), 6.67-6.62 (m, 2H), 6.48 (d, J = 7.4 Hz, 1H), 2.12 (s, 3H), 1.96 (s, 3H) ppm.
3g': Orange solid, m.p. = 258-259 °C; ^{1}H NMR (DMSO-d6, 300 MHz) δ =10.69 (s, 1H), 10.66 (s, 2H), 7.36 (d, J = 7.4 Hz, 1H), 7.20-7.18 (m, 2H), 6.90-6.86 (m, 5H), 6.67-6.64 (m, 2H), 6.18 (s, 1H), 6.12 (s, 1H), 1.94 (s, 6H) ppm .

2.4 Recovering and reusing of PVIm

PVIm was filtered and washed with hot ethanol (2 × 5 mL) and then dried overnight at 80 ºC by a vacuum oven. The study of FT-IR spectra of fresh and 4th recovered PVIm demonstrated the chemical and thermal stability of PVIm during the reaction, workup, and recycling conditions.

3.0 Results and discussion

Developing cost-effective and eco-friendly processes and performing reactions with safe and greener reagents, solvents, and catalysts are crucial issues of organic synthesis research. In

continuation of our recent studies [35-37], herein, the efficient catalytic activity of PVIm, as a functional polymer, for the synthesis of various bis(3-indolyl)methanes (BIMs) is described. Initially, the synthesis of BIMs was carried out in different solvents using PVIm, and the results are summarized in Table 1. These results suggest that solvent-free was the best condition for the synthesis of BIMs. It may be because polar protic solvents tend to inactive the base sites, and polar aprotic solvents tend to favor attack at the nitrogen, whereas nonpolar solvents prefer C-3 attack.

Table 1. Optimization of the solvent effect on the model reaction.[a]

Entry	Solvent	Yield [b] (%)
1	Dichloromethane	45
2	Toluene	55
3	Acetonitrile	50
4	Ethanol	21
5	Methanol	22
6	Solvent-free	60[c]

[a] Reaction condition: 4-chlorobenzaldehyde (1.0 mmol), indole (2.0 mmol), PVIm (10 mg), temperature (reflux), reaction time (2 h).

[b] Determined by GC.

[c] Reaction condition: 4-chlorobenzaldehyde (1.0 mmol), indole (2.0 mmol), PVIm (10 mg), temperature (80 °C), reaction time (2 h).

Then, the effect of the catalyst loading was studied on the model reaction. As shown in Table 2, the catalytic efficiency of PVIm enhanced in the presence of more amount of the catalyst, and the best result was observed with 20 mg of the catalyst loading (14 wt. % per 4-chlorobenzaldehyde), which afforded the desired product 3b in 95% yield. No improvement was observed in the product yield using more catalyst loading above 20 mg of PVIm. In the case of PVIm, the catalytic activity can be mainly attributed to the basicity of free imidazole rings attached to the backbone of the functional polymer. The pKa value of PVIm was estimated at around 6.0 [31]. A linear relationship was observed between the catalyst loading and 3b yield at a range of 5 mg to 20 mg of PVIm.

Table 2. Screening of PVIm loading in the model reaction.[a]

Entry	Amount of poly(4-vinylpyridine) (mg)	Yield [b] (%)
1	-	No reaction
2	5	41
3	10	60
4	20	95
5	30	96
6	40	96

a Reaction condition: 4-chlorobenzaldehyde (1.0 mmol), indole (2.0 mmol), temperature (80 °C), reaction time (2 h).

b Determined by GC.

The substrate scope of the new catalytic process was investigated by the reaction of various carbonyl compounds (1) with indole (2a) and 2-methylindole (2b) under optimized reaction conditions (Scheme 1).

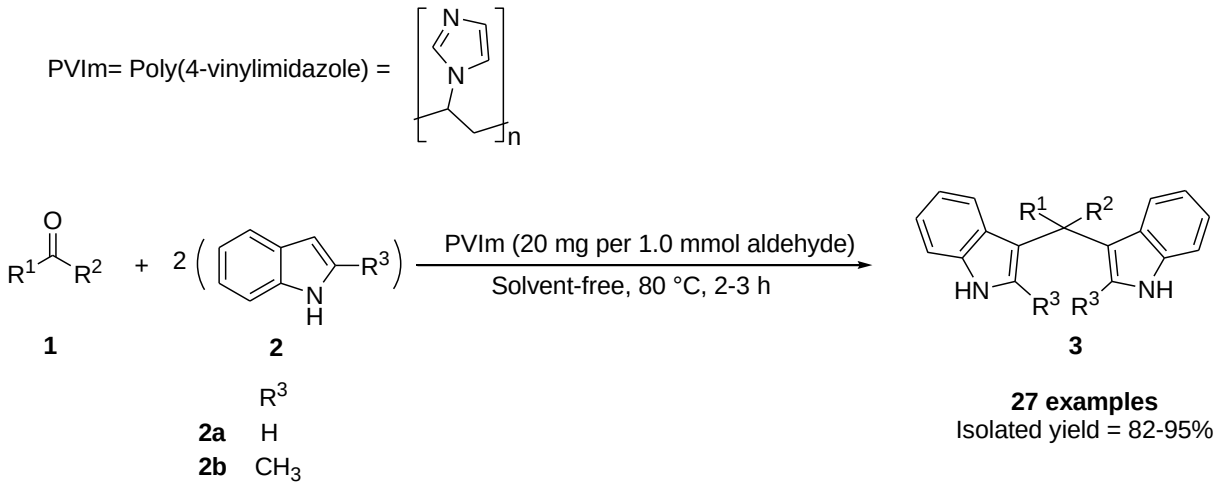

Scheme 1. Synthetic conditions of BIMs using PVIm.

Table 3. The substrate scope of the new catalytic process for the synthesis of BIMs.[a]

Entry	Aldehyde	R^3	Product	Time (min)	Yield (%)[b]	M.p. (°C)	
						Found	Reported (43)
1	C_6H_5-CHO	H	3a	135	94	127-128	123-125
2	4-Cl-C_6H_4-CHO	H	3b	120	95	87-88	87-89
3	2-Cl-C_6H_4-CHO	H	3c	124	93	76-78	77-78
4	4-CH_3O-C_6H_4-CHO	H	3d	135	90	191-192	195
5	3,4-$(CH_3O)_2$-C_6H_4-CHO	H	3e	140	90	200-201	197-199
6	4-CH_3-C_6H_4-CHO	H	3f	120	93	96-97	99-100
7	4-NO_2-C_6H_4-CHO	H	3g	120	95	243-244	245-246
9	4-Br-C_6H_4-CHO	H	3h	125	95	110-111	111-113
10	C_6H_5-CH=CH-CHO	H	3i	135	91	99-100	100-102
11	Furfural	H	3j	120	95	320-321	322-324
12	4-OH-C_6H_4-CHO	H	3k	135	90	208-209	210-212
13	2-OH-C_6H_4-CHO	H	3l	145	89	100-101	103-105
14	$CH_3CH_2CH_2CHO$	H	3m	165	90	Oil	Oil
15	$CH_3(CH_2)_5CHO$	H	3n	160	91	65-66	68-70
16	C_6H_5-CO-CH_3	H	3o	180	82	167-168	169-171
17	4-Cl-C_6H_4-CO-CH_3	H	3p	175	84	108-109	109-110
18	4-NO_2-C_6H_4-CO-CH_3	H	3q	170	89	271-272	274-276
19	Indol-3-carbaldehyde	H	3r	140	94	243-244	245-247
20	Isatin	H	3s	140	94	> 300	244-245
21	C_6H_5-CHO	CH_3	3a'	140	94	239-240	244-246
22	3,4-$(CH_3O)_2$-C_6H_4-CHO	CH_3	3b'	160	90	200-201	204-206
23	4-NO_2-C_6H_4-CHO	CH_3	3c'	140	95	242-243	240-242
24	4-OH-C_6H_4-CHO	CH_3	3d'	155	89	237-238	240-242
25	4-CH_3-C_6H_4-CHO	CH_3	3e'	135	91	179-180	175-177
26	Isatin	CH_3	3f'	160	91	298-299	300-301
27	Indol-3-carbaldehyde	CH_3	3g'	165	90	258-259	260-262

a The desired products were characterized by comparing their melting point and/or 1H NMR spectra with those of the known compounds.

b Isolated yield.

As seen in Table 3, a variety of substituted aromatic and heteroaromatic aldehydes smoothly reacted with indole (2a) or 2-methylindole (2b) using PVIm as a heterogeneous catalyst under the optimized reaction conditions, and the respective BIMs were isolated in 82-95% within 2-3 h.

Table 4. The superiority of our catalytic process for the preparation of 3,3'-bis-indolylphenylmethane compared with some previously reported methods.

Entry	Catalyst	Reaction condition	Time (min)	Catalyst loading	Yield (%)[a]	Ref.
1	CAN	CH_3CN (N_2 atm)	30	0.3 mol	89	44
2	Lanthanide triflate	EtOH / H_2O	720	0.1M solution	95	45
3	Acetic acid	H_2O	10 days	0.01 mol	71	46
4	Indium trichloride	CH_3CN	240	0.2 mol	96	47
5	Zeokarb-225	CH_3CN	450	0.5 g	95	48
6	[Hmim]HSO_4	EtOH	60	0.01 mol	97	14
7	Aminosulfonic acid	EtOH/H_2O (N_2 atm)	30	1.5 mol	93	49
8	Ammonium chloride	Solvent-free	120 h	0.5 mol	96	50
9	Poly(*N*-vinylimidazole)	Solvent-free (80 °C)	135 min	20 mg	94	This work

a Isolated yield.

Based on previously reported mechanisms in the literature [14, 46], a schematic reaction route was proposed, as shown in Scheme 2.

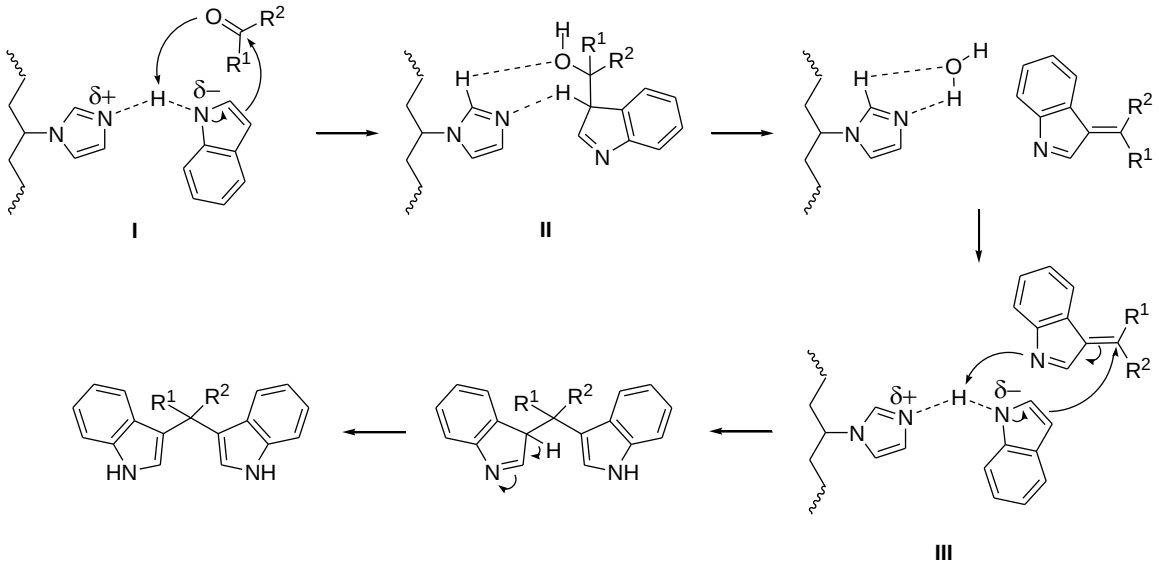

Scheme 2. A plausible mechanism of the synthesis of bis(3-indolyl)methanes in the presence of a catalytic amount of PVIm.

The reusability was investigated to show the worth of PVIm as an easy separable and recyclable heterogeneous catalyst. For this purpose, the model reaction was carried out several times consecutively. The first run gave the conversion of 95% after two hours. Then, the catalyst was collected by filtration, washed with Et2O and acetone, and dried at room temperature overnight. The subsequent runs were carried out in the same procedures four times, and the catalytic activity of PVIm remained almost constant, as shown in Table 5.

Table 5. Reusability of PVIm

Run	Time (min)	Isolated yield (%)
1	120	95
2	120	95
3	126	93
4	126	92

Conflicts of interest

There are no conflicts to declare.

Acknowledgements

This work was partially supported by a Research Grant (IF065-2020) from the Universiti Malaya, Malaysia. We are thankful to Sari Agricultural Sciences and Natural Resources University, Iran, and the Universiti Malaya, Malaysia, for the partial support of this work.

References

1. A. El-Gamal, W. L. Wang, C. Y. Duh, Sulfur-containing polybromoindoles from the formosan red alga Laurencia brongniartii. J. Nat. Prod. 2005, 68, 815-817.
2. T. Endo, M. Tsuda, J. Fromont, J. Kobayashi, A. Hyrtinadine, a bis-indole alkaloid from a marine sponge. J. Nat. Prod. 2007, 70, 423-424.
3. T. R. Garbe, M. Kobayashi, N. Shimizu, N. Takesue, M. Ozawa, H. Yukawa, Indolyl carboxylic acids by condensation of indoles with alpha-keto acids. J. Nat. Prod. 2000, 63, 596-598.
4. N. Sirisoma, A. Pervin, J. Drewe, B. Tseng, S. X. Cai, Discovery of substituted N'-(2-oxoindolin-3-ylidene)benzohydrazides as new apoptosis inducers using a cell- and caspase-based HTS assay. Bioorg. Med. Chem. Lett. 2009, 9, 2710-2713.
5. G. W. Gribble, In Comprehensive Heterocyclic Chemistry, vol. 2, second ed., Pergamom Press, New York, 1996, pp. 211.

6. B. P. Bandgar, K. A. Shaikh, Molecular iodine-catalyzed efficient and highly rapid synthesis of bis(indolyl)methanes under mild conditions. Tetrahedron Lett. 2003, 44, 1959-1961.

7. J. M. Frost, M. J. Dart, K. R. Tietje, T. R. Garrison, G. K. Grayson, A. V. Daza, O. F. E-Kouhen, L. N. Miller, L. Li, B. B. Yao, G. C. Hsieh, M. Pai, C. Z. Zhu, Antinociceptive (aminoalkyl)indoles. J. Med. Chem. 2008, 51, 1904-1912.

8. M. C. Pirrung, Z. Li, E. Hensley, Y. Liu, A. Tanksale, B. Lin, A. Pai, N. J. G. Webster, Parallel synthesis of indolylquinones and their cell-based insulin mimicry. J. Comb. Chem. 2007, 9, 844-854.

9. M. A. Zeligs, Diet and estrogen status: The cruciferous connection. J. Med. Food 1998, 1, 67-82.

10. B. Pal, V. S. Giri, P. Jaisankar, First indium trichloride catalyzed self-addition of indoles: One pot synthesis of indolylindolines. Catal. Commun. 2005, 6, 711-715. doi: 10.1016/j.catcom.2005.07.003

11. B. P. Bandgar, A. V. Patil, V. T. Kamble, Fluoroboric acid adsorbed on silica gel catalyzed synthesis of bisindolyl alkanes under mild and solvent-free conditions. Arkivoc 2007, 16, 252-259.

12. M. L. Deb, P. J. Bhuyan, Uncatalyzed Michael addition of indoles: synthesis of some novel 3-alkylated indoles via a three-component reaction in solvent-free conditions. Tetrahedron Lett. 2007, 48, 2159-2163.

13. A. Hasaninejad, A. Zare, H. Sharghi, K. Niknam, M. Shekouhy, P2O5/SiO2 as an efficient, mild, and heterogeneous catalytic system for the condensation of indoles with carbonyl compounds under solvent-free conditions. Arkivoc 2007, 14, 39-50.

14. J. T. Li, H. G. Dai, W. Z. Xu, T. S. Li, An efficient and practical synthesis of bis(indolyl)methanes catalyzed by aminosulfonic acid under ultrasound. Ultrason. Sonochem. 2006, 13, 24-27.

15. J. S. Yadav, B. V. S. Reddy, B. Padmavani, M. K. Gupta, Gallium(III) halide-catalyzed coupling of indoles with phenylacetylene: synthesis of bis(indolyl)phenylethanes. Tetrahedron Lett. 2004, 45, 7577-7579.

16. M. Karthik, C. J. Magesh, P. T. Perumal, M. Palanichamy, B. Arabindoo, V. Murugesan, Zeolite-catalyzed ecofriendly synthesis of vibrindole A and bis(indolyl)methanes. Appl. Catal. A Gen. 2005, 286, 137-141.

17. C. J. Magesh, R. Nagarajan, M. Karthik, P. T. Perumal, Synthesis and characterization of bis(indolyl)methanes, tris(indolyl)methanes and new diindolylcarbazolylmethanes mediated by Zeokarb-225, a novel, recyclable, eco-benign heterogenous catalyst. Appl. Catal. A Gen. 2004, 266, 1-10.

18. S. Palaniappan, A. John, Facile synthesis of bis(indolyl)methanes using polyindole salt as reusable catalyst. J. Mol. Catal. A Chem. 2005, 242, 168-172.

19. S. J. Ji, S. Y. Wang, Y. Zhang, T. P. Loh, Facile synthesis of bis(indolyl)methanes using catalytic amount of iodine at room temperature under solvent-free conditions. Tetrahedron 2004, 60, 2051-2055.

20. M. Chakraborty, N. Ghosh, R. Basak, Y. Harigaya, Dry reaction of indoles with carbonyl compounds on montmorillonite K10 clay: a mild, expedient synthesis of diindolylalkanes and vibrindole A. Tetrahedron Lett. 2002, 43, 4075-4078.

21. X. F. Zeng, S. J. Ji, S. Y. Wang, Novel method for synthesis of unsymmetrical bis(indolyl)alkanes catalyzed by ceric ammonium nitrate (CAN) under ultrasonic irradiation. Tetrahedron 2005, 61, 10235-10241.

22. S. Ko, C. Lin, Z. Tu, Y. F. Wang, C. C. Wang, C. F. Yao, CAN and iodine-catalyzed reaction of indole or 1-methylindole with α,β-unsaturated ketone or aldehyde. Tetrahedron Lett. 2006, 47, 487-492.

23. S. Kobayashi, M. Araki, M. Yasuda, One-pot synthesis of β-amino esters from aldehydes using lanthanide triflate as a catalyst. Tetrahedron Lett. 1995, 36, 5773-5776.

24. L. Wang, J. H. Han, T. Sheng, J. Z. Fan, X. Tang, Rare earth perfluorooctanoate [RE(PFO)3]-catalyzed condensations of indole with carbonyl Compounds. Synlett 2005, 337-339.

25. X. Li, J. Y. Wang, W. Yu, L. M. Wu, PtCl2-catalyzed reactions of o-alkynylanilines with ethyl propiolate and dimethyl acetylenedicarboxylate. Tetrahedron 2009, 65, 1140-1146.

26. X. Mi, S. Luo, J. He, J. P. Cheng, Dy(OTf)3 in ionic liquid: an efficient catalytic system for reactions of indole with aldehydes/ketones or imines. Tetrahedron Lett. 2004, 45, 4567-4570.

27. S. V. Ley, I. R. Baxendale, R. N. Bream, P. S. Jackson, A. G. Leach, D. A. Longbottom, M. Nesi, J. S. Scott, R. I. Storer, S. J. Taylor, Multi-step organic synthesis using solid-supported reagents and scavengers: a new paradigm in chemical library generation. J. Chem. Soc. Perkin Trans. 1 2000, 3815-4195.

28. M. G. Chung, H. W. Kim, B. R. Kim, Y. B. Kim, Y. H. Rhee, Biocompatibility and antimicrobial activity of poly(3-hydroxyoctanoate) grafted with vinyl imidazole. Int. J. Biol. Macromol. 2012, 50, 310-316.

29. I. C. Alupei, M. Popa, A. Bejenariu, S. Vasiliu, V. Alupei, Composite membranes based on gellan and poly(N-vinylimidazole). Synthesis and characterization. Eur. Polym. J. 2006, 42, 908-916.

30. C. Fodor, J. Bozi, M. Blazsó, B. Iván, Thermal behavior, stability, and decomposition mechanism of poly(N-vinylimidazole). Macromolecules 2012, 45, 8953-8960.

31. E. E. B. Anderson, T.E. Long, Imidazole- and imidazolium-containing polymers for biology and material science applications. Polymer 2010, 51, 2447-2454.

32. A. Horta, M. J. S. Molina, M. R. Gómez-Antón, I. S. F. Piérola, The pH inside a pH-sensitive gel swollen in aqueous salt solutions: poly(N-vinylimidazole). Macromolecules 2009, 42, 1285-1292.

33. N. Pekel, O. Güven, Separation of heavy metal ions by complexation on poly(N-vinylimidazole) hydrogels. Polym. Bull. 2004, 51, 307-314.

34. H. Bessbousse, T. Rhlalou, J. F. Verchère, L. Lebrun, Mercury removal from waste water using a poly(vinylalcohol)/poly(vinylimidazole) complexing membrane. Chem. Eng. J. 2010, 164, 37-48.

35. N. G. Khaligh, N.G. Poly(N-vinylimidazole) as an efficient catalyst for acetylation of alcohols, phenols, thiols and amines under solvent-free conditions. RSC Adv. 2013, 3, 99-110.

36. N. G. Khaligh, T. Mihankhah, Aldol condensations of a variety of different aldehydes and ketones under ultrasonic irradiation using poly(N-vinylimidazole) as a new heterogeneous base catalyst under solvent-free conditions in a liquid-solid system. Chin. J. Catal. 2013, 34, 2167-2173.

37. N. G. Khaligh, Poly(N-vinylimidazole) as a halogen-free and efficient catalyst for N-Boc protection of amines under solvent-free conditions. RSC Adv. 2012, 2, 12364-12370.

38. I. P. Beletskaya, E. A. Tarasenko, A. R. Khokhlov, V. S. Tyurin, Poly(N-vinylimidazole) as an efficient and recyclable catalyst of the aza-Michael reaction in water. Russ. J. Org. Chem. 2010, 46, 461-467.

39. Z. Chen, J. Yang, D. Yin, Y. Li, S. Wu, J. Lu, J. Wang, Fabrication of poly(1-vinylimidazole)/mordenite grafting membrane with high pervaporation performance for the dehydration of acetic acid. J. Membr. Sci. 2010, 349, 175-182.

40. A. H. Tian, J. -Y. Kim, J. Y. Shi, K. Kim, Poly(1-vinylimidazole)/Pd-impregnated Nafion for direct methanol fuel cell applications. J. Power Sources 2008, 183, 1-7.

41. K. Yao, Z. Wang, J. Wang, S. Wang, Biomimetic material-poly(N-vinylimidazole)-zinc complex for CO2 separation. Chem. Commun. 2012, 48, 1766-1768.

42. L. Cheng, P. –B. Zhang,Y. –F. Zhao, L. –P. Zhu, B. –K. Zhu,Y. -Y. Xu, Preparation and characterization of poly(N-vinylimidazole) gel-filled nanofiltration membranes. J. Membrane Sci. 2015, 492, 380-391.

43. F. Shirini, N. G. Khaligh, Succinimide-N-sulfonic acid catalyzed synthesis of bis(indolyl)methane and coumarin derivatives under mild conditions. Chin. J. Catal. 2013, 34,1890-1896.

44. C. Ramesh, N. Ravindranath, B. Das, Electrophilic substitution reactions of indoles with carbonyl compounds using ceric ammonium nitrate: A novel and efficient method for the synthesis of di- and tri-indolylmethanes. J. Chem. Res. (S) 2003, 72-74.

45. M. Xia, S. Wang, W. Yuan, Lewis acid catalyzed electrophilic substitution of indole with aldehydes and Schiff's bases under microwave solvent-free irradiation. Synth. Commun. 2004, 34, 3175-3182.

46. A. Kamal, A. A. Qureshi, Syntheses of some substituted di-indolylmethanes in aqueous medium at room temperature. Tetrahedron 1963, 19, 513-520.

47. G. Babu, N. Sridhar, P. T. Perumal, A Convenient Method of Synthesis of Bis-Indolylmethanes: Indium trichloride catalyzed reactions of indole with aldehydes and Schiff's bases. Synth. Commun. 2000, 30, 1609-1614.

48. D. G. Gu, S. J. Ji, Z. Q. Jiang, M. F. Zhou, T. P. Loh, An efficient synthesis of bis(indolyl)methanes catalyzed by recycled acidic ionic liquid. Synlett 2005, 959-962.

49. J. Azizian, F. Teimouri, M. R. Mohammadizadeh, Ammonium chloride catalyzed one-pot synthesis of diindolylmethanes under solvent-free conditions. Catal. Commun. 2007, 8, 1117-1121.

50. G. V. M. Sharma, J. J. Reddy, P. S. Lakshmi, P. R. Krishna, A versatile and practical synthesis of bis(indolyl)methanes/bis(indolyl)glycoconjugates catalyzed by trichloro-1,3,5-triazine. Tetrahedron Lett. 2004, 45, 7729-7732.

51. J. Brandrup, E. H. Immergut, E. Grulke, Solution Properties, in Polymer Handbook, Wiley, New York, 4th edn, 1999.

Malaysian Catalysis-An International Journal

Malay. Catal. Int. J Vol 1 (2021) 26-35

OVERVIEW

Photoelectrochemical water splitting process using titanium dioxide photocatalyst: A brief overview

Chin Wei Lai*[a] Jenny Hui Foong Chau [a]

a. Nanotechnology and Catalysis Research Centre (NANOCAT), Level 3, Block A, Institute for Advanced Studies (IAS), University of Malaya (UM), 50603 Kuala Lumpur, Malaysia

Received 28th June 2021,
Accepted 27th Sept 2021

DOI: 10.22452/mcij.vol1no1.3

Corresponding author:
cwlai@um.edu.my

Abstract

Hydrogen (H_2) has proved itself as a viable future energy carrier and alternative for fossil fuel in terms of ensuring a clean and sustainable energy supply. However, H_2 must be made available at a lower cost so that everyone can benefit from it and prevent causing a worldwide ecological imbalance. The usage of photoelectrochemical water splitting (PEC) technology by using TiO_2 photocatalyst can produce H_2 using renewable solar energy. The essential milestones, as well as the mechanism in PEC H_2 generation, are discussed in this article.

Keywords: Photoelectrochemical cell, Solar illumination, Water splitting

1. Introduction

Nowadays, a variety of environmental problems affect our world. The increased growth in human population and industrial development has resulted in the generation of various waste products and high consumption of energy. As a result, developing a continuous, renewable, and clean energy supply to protect the environment by reducing pollution emissions is the most pressing concern for human civilization. H2 is now widely regarded as an ideal future energy carrier [1], [2]. The energy yield of H2 is approximate 122 kJ/g which this provided energy is larger than the energy provided by conventional hydrocarbon fossil fuels combustion [3]. Besides, the process to provide energy through H_2 combustion is environmental friendly due to the harmless end product of H_2O [4]. H_2 can be generated through various methods using different raw materials, including fossil fuels and biomass [3], [5]. However, these methods contribute to problems such as energy depletion, environmental pollution, production of unwanted CO_2, the need for huge electrical consumption, and low efficiency of H_2 production [3], [5], [6]. Therefore, a suitable method must be invented to resolve all the disadvantages.

Solar energy is the largest, clean, renewable, and free energy source accessible throughout the world providing up to 1.2 x 10^{14} kJ of energy per second [7-8]. The amount of solar energy reaching our planet is approximately 100000 TW of which 36000 TW reaches land surface each year [9]. PEC water splitting is one of the most widely used techniques that use sunlight energy to separate water molecules into H_2 and oxygen (O_2) molecules ($2H_2O \rightarrow 2H_2 + O_2$) and thus reduce electrical energy consumption [8-10]. This technique is effective and environment friendly to make it the most promising method for H_2 production so far. In this method, H_2 and O_2 are going to be generated at two separated photoelectrodes, anode and cathode, respectively. Large varieties of semiconductor (metal oxide) materials are used as photocatalysts in the PEC water splitting process. Photocatalysts activated by solar irradiation produce photogenerated electrons and holes, and they will react with water to generate H_2 and O_2 effectively [1], [9].

In this article, some of the early studies in heterogeneous photocatalysis start from solar photovoltaic to the solar H_2 in PEC water splitting cell will be reviewed. The development of a TiO_2 semiconductor photocatalyst capable of producing H_2 efficiently through both the PEC cell and light activation will be reviewed.

2. Historical overview of PEC application

As the demand for alternative energy sources grows worldwide, there is an increasing interest in cost-effective, conveniently produced energy sources with excellent performance. Alexandre Edmond Becquerel's early experiment based on photocatalysis was published in 1839 [11]. He discovered that an electrode made of silver chloride (AgCl) coupled to a counter electrode immersed in an aqueous electrolyte creates an electrical current and voltage during solar light irradiation. The discovery of capturing solar energy and turning it to electrical power sparked a slew of new ideas for scientists and academics looking for alternate energy sources. The photoelectric effect was then applied to a device for the first time in 1883 by Charles Fritts, who created a gold and selenium n-p junction device with a 1 percent efficiency [12]. There was a scarcity of information about heterogeneous photocatalysis in the early twentieth century.

Bell Laboratories published and reported the first p-n junction solar cell design in 1954, with a 6 percent efficiency [13]. Bell Labs' breakthrough resulted in the first commercially practical solar cell and revolutionized the photovoltaic industry. Improvements have been made to make photovoltaic more accessible in the global market. Solid-state junction devices built of silicon have

dominated the conversion of solar energy to electrical power. The most significant disadvantage of photovoltaics is that it does not work when the sun is not strong or in bad weather. As a result, energy storage is critical, which can be accomplished by creating H_2 and storing the energy as chemical energy in H_2. The stored energy is then can be released as electrical energy when needed. PEC cells have typically relied on nanocrystal structure materials. The nanostructure material is having many advantages such as high current generation efficiency, low cost, and chemical stability [14].

In 1972, Fujishima and Honda discovered the PEC H_2 production using TiO_2 electrodes [15-17]. Because crude oil prices had abruptly risen and a future shortage of crude oil was a real issue, this event heralded the start of a new era in heterogeneous photocatalysis. As a result, scientific interests in semiconductor photocatalysis based on TiO_2 photocatalyst have grown significantly. To have a better understanding of the fundamental mechanisms and to improve the photocatalytic effectiveness of TiO_2, research works have been published. TiO_2 has emerged as the top candidate for PEC cells due to characteristics such as non-toxicity, low cost, excellent stability against photo-corrosion, potent photocatalytic activity, and self-cleaning ability [16-18].

In the early 1980s, TiO_2 in different forms such as solution suspension and solid photoelectrode was used to generate H_2 through the PEC cell. However, this system has several flaws such as the appearance of trapping sites, long travel distances, and disordered contact areas between two particles or spheres. Therefore, the electron transporting time in the TiO_2 bulk phase is relatively long, resulting in the scattering of free electrons with lower mobility. These drawbacks reduce the performance of PEC cells. Other than that, an appropriate substrate is needed to support the particles or spheres in the PEC system and a filtration process might be needed after using them [17], [19].

In the early 1990s, TiO_2 thin film photocatalyst was created in the PEC application because it provides a more resilient and cost-effective solution by removing the issues mentioned above and being reusable in the PEC application. However, thin-film photocatalysts do not have a significantly large surface area [20]. To achieve optimum overall efficiency without increasing the geometric area, it is critical to maximizing the active sites of TiO_2 thin films. Advanced geometries of TiO_2 thin films have recently garnered much attention, especially nanostructured TiO_2, which has a large surface area (active sites) for photon absorption in PEC application [17].

Zwiling and co-researchers reported the first generation of self-organized porous TiO_2 by anodizing Ti foil in chromic acid electrolytes containing hydrofluoric acid (HF) in 1999 [16]. Gong and his research team later constructed self-organized TiO_2 nanotubes arrays with excellent uniformity by anodizing Ti in an aqueous dilute HF electrolyte in 2001. The maximum nanotube lengths were approximately 500 nm. One-dimensional (1D) nanostructured TiO_2 film can be simply removed and replaced after the photocatalytic process. Therefore, 1D nanostructured TiO_2 film is used in photoreactors for cost-effective purposes. Various methodologies such as hydrothermal, sol-gel, and anodization can be used to create 1D TiO_2 nanostructures [16], [21–23].

TiO_2 nanotubes have recently been identified as a possible building element for a new generation of nanoscale devices. Self-organized TiO_2 nanotube arrays bring much attention, not only because of their variable band gap due to the quantum confinement effect but also because of their larger surface area which allows for more photon absorption [15], [17]. However, a suitable method to produce nanotubes arrays must be researched and different effects such as wall thickness, length, pore width, and intertube spacing must be optimized to obtain preferred dimensions and morphologies. Many researchers have found that highly ordered TiO_2 nanotubes are superior and highly efficient in PEC responses due to their higher surface area allows for better light scattering and thus more electron generation [17]. The improvement of charge transport favors PEC features that improve photocurrent resulting in more efficient H_2 generation. As a result, TiO_2 nanotubes have been proved to be a stable photocatalyst or semiconductor for efficient light absorption in water photo-electrolysis reactions.

3. Principle and mechanism of PEC water splitting

The main components of PEC water splitting device are made up of semiconductor photoelectrodes which can absorb light, electrolyte, and separation membrane. There are three main processes involved in a complete PEC water splitting process. The first process is light absorption by semiconductor photoelectrode. Different semiconductors are having different band gap energies. Band gap reading is the difference between the valence band (highest occupied molecular orbital) and conduction band (lowest unoccupied molecular orbital) of the semiconductor [9]. A pair of charge carriers is generated when the semiconductor material received photons (from sunlight irradiation) with energies larger than its band gap energy. Excited

electrons located in the valence band will tend to move to the conduction band and leaving holes in the valence band. In the water splitting process, the valence band potential of the semiconductor must be positive than the O_2/H_2O redox potential of 1.23 V vs. NHE (pH = 0) and the conduction band potential must be more negative than the H^+/H_2 redox potential of 0 V vs. NHE to carry out water oxidation and reduction reactions respectively [9], [10], [16].

The second process is the separation and transportation of photoexcited charge carriers. The third process is the redox reactions of water splitting. Fig. 1 demonstrates the set-up of a simple PEC device (type I) based on n-type semiconductor as the photoanode where (I) to (III) represent first to third processes. In this type, I PEC device, a single semiconductor can be used either as a photoanode or photocathode to carry out water oxidation or reduction process.

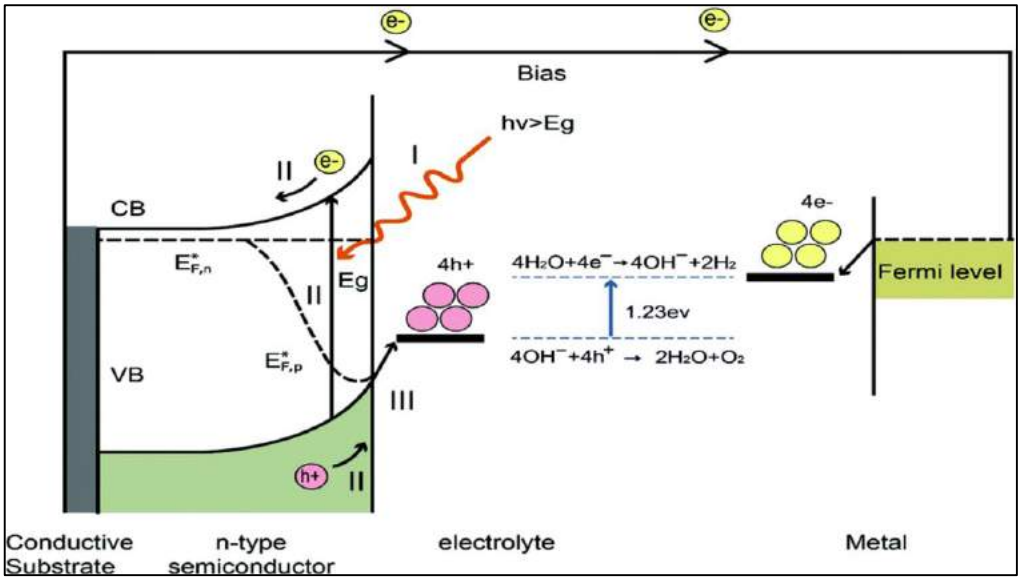

Fig. 1 Type I PEC cell with n-type semiconductor as photoanode and metal as the counter electrode. Reproduced from [9] with permission from the Royal Society of Chemistry.

Metal oxide has gotten much attention in PEC water splitting process due to benefits including chemical and physical stability, low cost, easy accessibility, wide varieties, etc. [10]. Despite all the advantages, the problems of weak electrical characteristics, large band gap reading, fast photogenerated electron, and holes recombination need to be solved to enhance the H_2 production in the water splitting process [18], [24]. Fig. 2 demonstrates different semiconductors together with their valence and conduction band edge readings. Band positions of the semiconductor depend on the pH of the electrolyte. It is important to research a low cost, efficient, high stability,

non-toxic, and easy to access material for PEC water splitting process. The suitable semiconductor used in the PEC systems must have four essential characteristics as shown below [9], [16-18]:

i. Photochemical stability:

   The material must be stable in an aqueous solution to avoid photo-corrosion during the photo-electrolysis reaction. Photo-corrosion occurs when the photoexcited charge carrier does not carry out water oxidation or reduction but instead decomposes the photocatalyst itself. Semiconductors such as zinc oxide, molybdenum disulfide, and bismuth vanadate are undergoing photo-corrosion easily.

ii. Band gap:

   Sunlight is made up of approximately 5% of UV light (wavelength of 300 to 400 nm), 43% of visible light (wavelength of 400 to 700 nm), and infrared radiation (wavelength of 700 to 2500 nm). Thus, the light absorption of the semiconductor must be within the visible region to enhance the efficiency of water splitting. The theoretical minimum band gap energy for PEC water splitting process is 1.23 eV (light absorption around the wavelength of 1100 nm) due to the O_2/H_2O redox potential as mentioned before. Besides, the possibility of both the thermodynamic energy losses during charge carrier transportation and overpotential requirement for surface reaction kinetics must be considered to evaluate suitable band gap energy reading. Thus, the semiconductor candidate must display a band gap energy of more than 1.8 eV (light absorption around 700 nm). The band gap reading should not be more than 3.2 eV due to the possibility of low sunlight intensity for wavelength under 390 nm considering the possibility of overpotential losses and the initial energy required to begin the water splitting reaction.

iii. Charge carrier separation and transportation

   The fast recombination rate of the charge carrier affects the water splitting efficiency. A study carried out by researchers shows that approximately 60-90% of photoexcited electrons recombine with holes within 10 ns.

iv. Energy level:

   The reduction and oxidation potential of the photocatalyst must lie between the conduction and valence band edges for the immediate water splitting reaction.

TiO_2, as mentioned in the previous section is widely used in this application due to its distinctive characteristics [18]. Fig. 3 displays the layout of a simple PEC water splitting set-up using TiO_2

photoanode and platinum photocathode. In Fig. 3, when TiO_2 is irradiated with light energy larger than its band gap energy, charge carriers are formed. The exciting form of electrons produced by TiO_2 will travel through the circuit towards the platinum electrode and undergoes a reduction process to synthesize H_2 while holes carry out an oxidation process to form O_2 [2], [16], [18]. The overall process is shown in Eq 1 to 3 as follow:

$$TiO_2 + 2\,h\nu \rightarrow TiO_2 + 2e^- + 2h^+ \quad (1)$$

$$2H_2O + 4h^+ \rightarrow O_2 + 4H^+ \quad (2)$$

$$2H^+ + 2e^- \rightarrow H_2 \quad (3)$$

However, TiO_2 can only absorb UV light due to its large band gap reading (approximate 3.2 eV for anatase and 3.0 eV for rutile phase). Besides, the fast recombination rate of photoexcited electron-hole pairs also affects their water splitting efficiency [15], [18]. Today, methods including doping with other metal or non-metal materials [25]–[29] and formation of binary [30], ternary [31], quaternary composite heterostructures [32] have been reported in numerous publications to promote more efficient charge separation, longer charge carrier lifetimes, and improved interfacial charge transfer in TiO_2. Furthermore, the recombination rate of electron-hole pairs can be enhanced by constructing a TiO_2 heterojunction photoanode [31]. Furthermore, the formation of this structure also improves the efficiencies of both the surface reaction kinetics and photo-redox process [31].

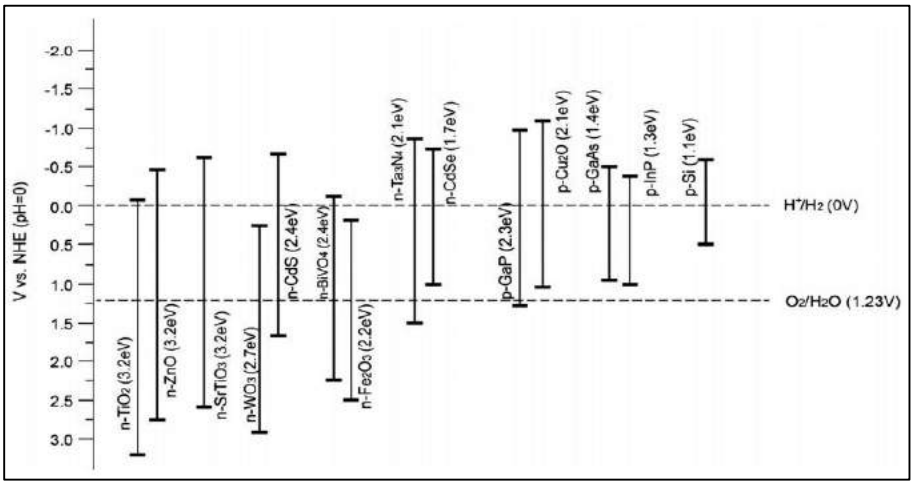

Fig. 2 Band positions of different semiconductors corresponding to the redox potential of water splitting at pH = 0. Reproduced from [9] with permission from the Royal Society of Chemistry.

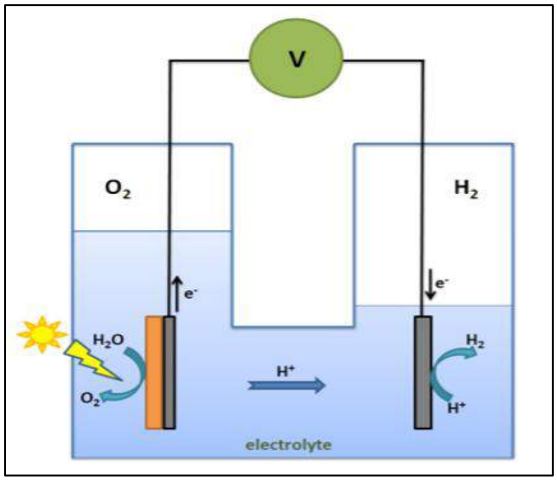

Fig. 3 PEC water splitting using TiO_2 photoanode and platinum photocathode. Reproduced with permission from [33].

4. Conclusion

All in all, this review sought to provide an overview of the metal oxide semiconductor in the PEC H_2 production application so that the reader may gain a better understanding of the historical context, basic fundamental investigations, and mechanism in PEC H_2 generation. TiO_2 photocatalyst can be used as the photoanode material in PEC cells to generate H_2 because of their distinctive characteristics such as low costs, chemically stability, long lifetime of charge carriers, powerful photocatalytic ability, high resistance towards photo-corrosion, and large surface area.

Acknowledgement

This research work was financially supported by Fundamental Research Grant Scheme FRGS/1/2020/TK0/UM/02/8 (No. FP023-2020), and Global Collaborative Programme – SATU Joint Research Scheme (No. ST004-2021).

References

1. Y. Zhang, Y. Bu, L. Wang, and J.-P. Ao, Regulation of the photogenerated carrier transfer process during photoelectrochemical water splitting: A review, Green Energy Environ. 2020, pp. 479-495

2. R. Singh and S. Dutta, A review on H_2 production through photocatalytic reactions using TiO_2/ TiO_2-assisted catalysts, Fuel, 2018, 220, pp. 607–620.

3. S. E. Hosseini and M. A. Wahid, Hydrogen production from renewable and sustainable energy resources: Promising green energy carrier for clean development, Renew. Sustain. Energy Rev., 2016, 57, pp. 850–866.

4. C. Acar and I. Dincer, Review and evaluation of hydrogen production options for better environment, J. Clean. Prod., 2019, 218, pp. 835–849.

5. P. Nikolaidis and A. Poullikkas, A comparative overview of hydrogen production processes, Renew. Sustain. Energy Rev., 2017,67, pp. 597–611.

6. V. TD, M. TS, dos S. DDRM, and C. AD, Hydrogen: Trends, production and characterization of the main process worldwide, Int. J. Hydrogen Energy, 2017, 42(4), pp. 2018–2033.

7. I. Roger, M. A. Shipman, and M. D. Symes, Earth-abundant catalysts for electrochemical and photoelectrochemical water splitting, Nat. Rev. Chem., 2017, 1(1), pp. 3.

8. R. Li *et al.*, Achieving overall water splitting using titanium dioxide-based photocatalysts of different phases, Energy Environ. Sci., 2015 8,(8), pp. 2377–2382.

9. C. R. Jiang, S. J. A. Moniz, A. Wang, T. Zhang, and J. Tang, Photoelectrochemical devices for solar water splitting – materials and challenges, Chem. Soc. Rev., 2017, 46(15), pp. 4645–4660.

10. N. Han et al., Perovskite and related oxide based electrodes for water splitting, J. Clean. Prod., 2021, 318, pp. 128544.

11. R. Michal, S. Sfaelou, and P. Lianos, Photocatalysis for renewable energy production using Photo Fuel Cells, Molecules, 2014, 19(12), pp. 19732–19750.

12. E. Kim, J. H. Park, and G. Han, Design of TiO2 nanotube array-based water-splitting reactor for hydrogen generation, J. Power Sources, 2008,184, pp. 284–287.

13. K. Yu and J. Chen, Enhancing Solar Cell Efficiencies through 1-D Nanostructures, Nanoscale Res. Lett., 2008, 4(1), pp. 1.

14. N. Baig, I. Kammakakam, and W. Falath, Nanomaterials: a review of synthesis methods, properties, recent progress, and challenges, Mater. Adv., 2021,.2(6), pp. 1821–1871.

15. F. X. Xiao and B. Liu, Plasmon-dictated photo-electrochemical water splitting for solar-to-chemical energy conversion: Current status and future perspectives, Adv. Mater. Interfaces, 2018, 5, pp. 1701098.

16. Y. Zhao, N. Hoivik, and K. Wang, Recent advance on engineering titanium dioxide nanotubes for photochemical and photoelectrochemical water splitting, Nano Energy, 2016, 30, pp. 728–744,

17. Y. Lan, Y. Lu, and Z. Ren, Mini review on photocatalysis of titanium dioxide nanoparticles and their solar applications, Nano Energy, 2013, 2(5), pp. 1031–1045.

18. A. Gellé and A. Moores, Water splitting catalyzed by titanium dioxide decorated with plasmonic nanoparticles, Pure Appl. Chem., 2017, 89 (12), pp. 1817-1827.

19. M. Jefferson, Sustainable energy development: Performance and prospects, Renew. Energy,

2006, 31, pp. 571–582.

20. L. C. Escaliante, K. O. Rocha, and J. H. D. Silva, Stability of the photocatalytic activity of TiO2 deposited by reactive Sputtering, Mater. Res., 24(1).

21. J. Cabrera, H. Alarcón, A. López, R. Candal, D. Acosta, and J. Rodríguez, Synthesis, characterization and photocatalytic activity of 1D TiO_2 nanostructures, Water Sci. Technol., 2014, 70, pp. 972–979.

22. M. Ge et al., A review of one-dimensional TiO2 nanostructured materials for environmental and energy applications, J. Mater. Chem. A, 2016, 4(18), pp. 6772–6801.

23. Q. Zhang et al., Anodic Oxidation Synthesis of One-Dimensional TiO_2 Nanostructures for Photocatalytic and Field Emission Properties, J. Nanomater., 2014, pp. 831752.

24. H. Sudrajat et al., Origin of the overall water splitting activity over Rh/Cr_2O_3@ anatase TiO_2 following UV-pretreatment, Int. J. Hydrogen Energy, 2021, pp. 31228-31238.

25. J. Cai, M. Zhou, X. Xu, and X. Du, Stable boron and cobalt co-doped TiO2 nanotubes anode for efficient degradation of organic pollutants, J. Hazard. Mater., 2020, 396.

26. X. Hou et al., Enhanced photoelectrocatalytic degradation of organic pollutants using TiO2 nanotubes implanted with nitrogen ions, J. Mater. Sci., 2020, 55(14), pp. 5843–5860.

27. A. Zada et al., Improved visible-light activities for degrading pollutants on TiO2/g-C3N4 nanocomposites by decorating SPR Au nanoparticles and 2,4-dichlorophenol decomposition path, J. Hazard. Mater., 2018, 342, pp. 715–723.

28. M. Coto et al., Tuning the properties of a black TiO2-Ag visible light photocatalyst produced by a rapid one-pot chemical reduction, Mater. Today Chem., 2017, 4, pp. 142–149.

29. S. A. Ansari, M. M. Khan, M. O. Ansari, and M. H. Cho, Silver nanoparticles and defect-induced visible light photocatalytic and photoelectrochemical performance of Ag@m-TiO2 nanocomposite, Sol. Energy Mater. Sol. Cells, 2015, 141, pp. 162–170.

30. Z. N. Kayani, A. Kamran, Z. Saddiqe, S. Riaz, and S. Naseem, Probe of ZrTiO2 thin films with TiO2-ZrO2 binary oxides deposited by dip coating technique, J. Photochem. Photobiol. B Biol., 2018, 183, pp. 357–366.

31. X. Shi et al., Facile construction TiO2/ZnIn2S4/Zn0.4Ca0.6In2S4 ternary hetero-structure photo-anode with enhanced photoelectrochemical water-splitting performance, Surfaces and Interfaces, 2021, 26, pp. 101323.

32. S. S. M. Bhat et al., Substantially enhanced photoelectrochemical performance of TiO2 nanorods/CdS nanocrystals heterojunction photoanode decorated with MoS2 nanosheets, Appl. Catal. B Environ., 2019, pp. 118102.

33. C. H. Liao, C. W. Huang, and J. C. S. Wu, Hydrogen production from semiconductor-based photocatalysis via water splitting, Catalysts, 2012, 2(4), pp. 490–516.